Phosphine-Induced Ancillary Ligand Orthometalation at a Tantalum−Tantalum Double Bond

Michael P. Shaver and Michael D. Fryzuk*

Department of Chemistry, University of British Columbia, 2036 Main Mall, Vancouver, British Columbia, V6T 1Z1 Canada

Received January 21, 2005

The dinuclear tantalum tetrahydride complexes (^{RPh}[NPN]Ta)$_2$(μ-H)$_4$ (^{RPh}[NPN] = (PhNSiMe$_2$-CH$_2$)$_2$PR; R = Ph, Cy) promote the asymmetric activation of molecular nitrogen to form (^{RPh}[NPN]Ta)$_2$(μ-η^1:η^2-N$_2$)(μ-H)$_2$. The coordinatively unsaturated dinuclear dihydride, (^{RPh}[NPN]Ta)$_2$(μ-H)$_2$, has been proposed as the reactive intermediate, with a tantalum−tantalum double bond storing four electrons with which to reduce N$_2$. Efforts to trap (^{CyPh}[NPN]Ta)$_2$(μ-H)$_2$ with excess PMe$_3$ at low temperatures promoted the formation of a green product, proposed to be (^{CyPh}[NPN]Ta(PMe$_3$))$_2$(μ-H)$_2$. Attempts to isolate this product promoted the orthometalation of an ancillary ligand N−Ph ring, forming ^{CyPh}[NPN]Ta(μ-H)$_2$[μ-N(C$_6$H$_4$)]Ta[PN](H)(PMe$_3$). Addition of 1 equiv of PMe$_3$ to (^{PhPh}[NPN]-Ta)$_2$(μ-H)$_4$ immediately produced the analogous orthometalation derivative, ^{PhPh}[NPN]-Ta(μ-H)$_2$[μ-N(C$_6$H$_4$)]Ta[PN](H)(PMe$_3$).

Introduction

The tantalum tetrahydride complexes (^{RPh}[NPN]Ta)$_2$-(μ-H)$_4$, (R = Cy, **1a**; R = Ph, **1b**) promote the coordination and activation of molecular nitrogen to give (^{RPh}[NPN]Ta)$_2$(μ-η^1:η^2-N$_2$)(μ-H)$_2$.[1,2] The asymmetrically bound N$_2$ fragment displays remarkable reactivity with main-group hydrides. Addition of boranes or silanes effects the formation of new N−B[3] and N−Si[4] bonds, respectively, and ultimately results in N−N bond cleavage of the coordinated dinitrogen. It is suspected that the reactive intermediate in the coordination and activation of N$_2$ is (^{RPh}[NPN]Ta)$_2$(μ-H)$_2$ (**2**), a dinuclear dihydride complex with a Ta=Ta double bond generated via reductive elimination of H$_2$, as shown in eq 1.

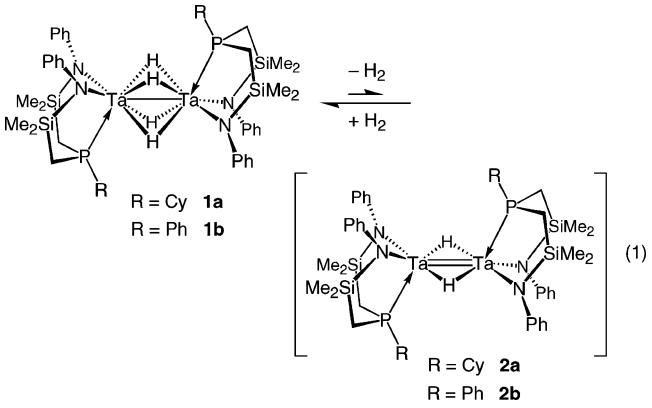

(1)

Indirect evidence for the intermediacy of the dihydride (^{RPh}[NPN]Ta)$_2$(μ-H)$_2$ was found in the reaction of **1a** and **1b** with primary and secondary phosphines. Isotopic labeling studies of P−H bond activation pointed toward **2** as possibly being involved.[5] Given that the dinuclear dihydride is coordinatively unsaturated, there is the possibility that it could be trapped by addition of suitable donors. The existence of the complex (Cl$_2$(PMe$_3$)$_2$-Ta)$_2$(μ-H)$_2$, a dinuclear dihydride Ta(III) complex with a Ta=Ta double bond, provides good support for this idea.[6] Other examples of reactive dinuclear Ta(III) complexes that contain Ta=Ta double bonds include (η^5-C$_5$Me$_4$R)$_2$Ta$_2$(μ-X)$_4$ (R = Me, Et; X = Cl, Br)[7−11] and thioether and phosphine adducts of Ta(III).[12−14] Reversible addition of H$_2$ has also been observed with ditungsten systems.[15]

In this work, we describe our attempts to generate phosphine adducts of the dinuclear tantalum dihydride **2**. What results is a phosphine-induced C−H activation of the N−Ph unit of the ancillary ligand.

* Corresponding author. E-mail: fryzuk@chem.ubc.ca.

(1) Fryzuk, M. D.; Johnson, S. A.; Rettig, S. J. *J. Am. Chem. Soc.* **1998**, *120*, 11024.
(2) Fryzuk, M. D.; Johnson, S. A.; Patrick, B. O.; Albinati, A.; Mason, S. A.; Koetzle, T. F. *J. Am. Chem. Soc.* **2001**, *123*, 3960.
(3) Fryzuk, M. D.; MacKay, B. A.; Johnson, S. A.; Patrick, B. O. *Angew. Chem., Int. Ed.* **2002**, *41*, 3709.
(4) Fryzuk, M. D.; MacKay, B. A.; Patrick, B. O. *J. Am. Chem. Soc.* **2003**, *125*, 3234.
(5) Shaver, M. P.; Fryzuk, M. D. *Organometallics* **2005**, *24*, 1419.
(6) Scioly, A. J.; Luetkens, M. L.; Wilson, R. B.; Huffman, J. C.; Sattelberger, A. P. *Polyhedron* **1987**, *6*, 741.
(7) Ting, C.; Baenziger, N. C.; Messerle, L. *J. Chem. Soc., Chem. Commun.* **1988**, 1133.
(8) Ting, C.; Messerle, L. *J. Am. Chem. Soc.* **1987**, *109*, 6506.
(9) Ting, C.; Messerle, L. *J. Am. Chem. Soc.* **1989**, *111*, 3449.
(10) Huang, J.; Lee, T.; Swenson, D.; Messerle, L. *Inorg. Chim. Acta* **2003**, *345*, 209.
(11) Huang, J.; Luci, J. J.; Lee, T.; Swenson, D. C.; Jensen, J. H.; Messerle, L. *J. Am. Chem. Soc.* **2003**, *125*, 1688.
(12) Messerle, L. *Chem. Rev.* **1988**, *88*, 1229.
(13) Cotton, F. A.; Daniels, L. M.; Murillo, C. A.; Wang, X. P. *Inorg. Chem.* **1997**, *36*, 896−902.
(14) Cotton, F. A.; Falvello, L. R.; Najjar, R. C. *Inorg. Chem.* **1983**, *22*, 375−377.
(15) Green, M. L. H.; Mountford, P. *J. Chem. Soc., Chem. Commun.* **1989**, 732−734.

10.1021/om050045e CCC: $30.25
Publication on Web 04/15/2005

Results and Discussion

Addition of triphenylphosphine to **1a** or **1b** gave no reaction. ^{31}P NMR in situ experiments showed only resonances due to free triphenylphosphine and unreacted tetrahydride; in addition, the characteristic deep purple color for solutions of **1a** and **1b** remained unchanged. Thermolysis of these mixtures did not promote complex formation; instead, protonation of the [NPN] ancillary ligand to form $^{RR'}$[NPN]H$_2$ was observed. Similarly, the bulky tertiary phosphines PBu$^t_3$ and PPr$^i_3$ did not exhibit any reactivity with the dinuclear tetrahydrides **1a** and **1b**.

Addition of an excess of sterically unencumbered trimethylphosphine to (^{CyPh}[NPN]Ta)$_2$(μ-H)$_4$, **1a**, produced a different result. Cooling a mixture of 8 equiv of PMe$_3$ and **1a** in Et$_2$O to approximately −80 °C resulted in the solution turning from deep purple to deep green. Upon warming the solution, the color reverted back to purple, indicative of the starting tetrahydride. As long as the solution is sealed, the color could be cycled simply by adjusting the temperature of the vessel.

Solution NMR studies of the green compound (d_8-toluene, −80 °C) showed broad resonances at −30 and +18 ppm in the ^{31}P{^{1}H} NMR spectrum, integrated against an external standard to be 2P each, lending support for the presence of the bis(trimethylphosphine) adduct **3a** (eq 2). Analysis of ^{1}H{^{31}P} spectra indicated a new broad resonance at 8.5 ppm, integrating to 2H against the SiMe resonances; this peak can be tentatively assigned to the two bridging hydrides. Also observed were broadened resonances for **1a** and free PMe$_3$. Efforts to extract equilibrium constants and thermodynamic data by following this transformation by variable-temperature NMR spectroscopy were complicated by a rearrangement process (vide infra).

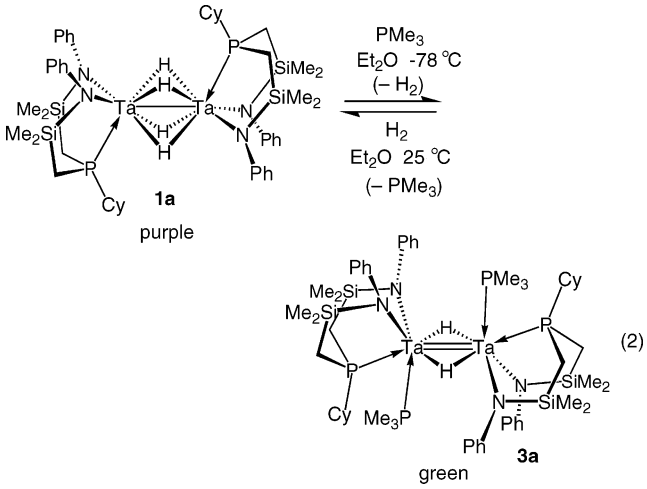

(2)

It can be assumed that the equilibrium in eq 2 is extremely small at room temperature and that the forward reaction is exothermic, as low temperatures and a large excess of trimethylphosphine are required to shift the equilibrium concentrations to the products. Attempts to drive the equilibrium to the right to increase the concentration of **3a** by removal of H$_2$ resulted in a new transformation.

Upon removal of H$_2$ at ambient temperatures, the solution turned from deep purple to red, not the anticipated green color of **3a**. Workup of the reaction

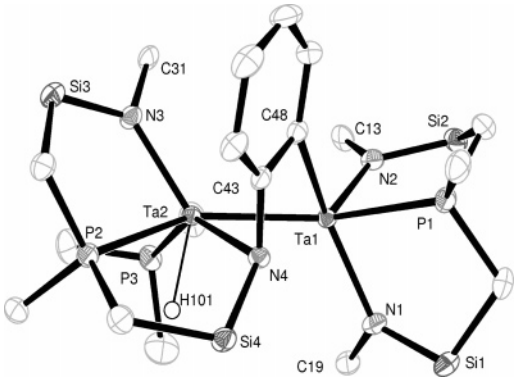

Figure 1. ORTEP drawing (spheroids at 50% probability) of **4a**. Silylmethyl, N-phenyl, and P-cyclohexyl ring carbons other than ipso and methine carbons have been omitted for clarity. The bond between N4 and Ta1 is not explicitly given.

mixture gave a red solid analyzed by ^{1}H, ^{31}P, ^{1}H/^{31}P HSQC, and ^{1}H/^{1}H COSY NMR experiments. Three resonances are observed in the ^{31}P{^{1}H} NMR spectrum: a doublet at −20.2 ppm (P$_A$, 1 P), a singlet at 10.5 ppm (P$_B$, 1 P), and a doublet at 13.8 ppm (P$_C$, 1 P). In the ^{1}H NMR spectrum, resonances assigned to eight SiMe environments overlap with a large resonance (9 H) coupling strongly to P$_A$, as observed in ^{1}H/^{31}P HSQC experiments. From coupling constant and chemical shift information, P$_A$ is likely a coordinated PMe$_3$ group. Cyclohexyl and methylene resonances couple to P$_B$ and P$_C$ in the ^{1}H/^{31}P HSQC spectrum, indicating P$_B$ and P$_C$ arise from the [NPN] ancillary ligand. These data are inconsistent with the anticipated symmetrical structure of the phosphine adduct **3a**. Also not consistent with **3a** was the observation of three separate hydride resonances at 5.06, 8.15, and 11.24 ppm, each of which is coupled to phosphorus-31: P$_A$ couples to H$_A$ at 5.06 ppm, P$_B$ couples to H$_B$ at 8.15 ppm, and P$_C$ couples to H$_C$ at 11.24 ppm. If it is assumed that the three peaks are all tantalum hydrides, the chemical shift of H$_A$ indicates it is likely bound terminally. H$_B$ and H$_C$ can be assigned with less certainty, but are most likely bridging hydrides.

Fortunately, single crystals of this red product containing 1.5 equiv of cocrystallized benzene were obtained, which allowed analysis by X-ray diffraction experiments. An ORTEP[16] depiction of the solid-state molecular structure of **4a** is shown in Figure 1; this transformation is also shown schematically in eq 3.

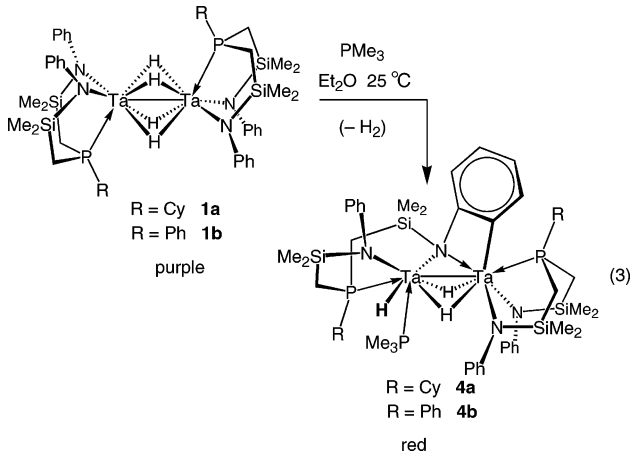

(3)

Table 1. Selected Bond Distances (Å) and Angles (deg) for 4a

lengths		angles		angles	
Ta(2)−N(3)	2.145(3)	N(3)−Ta(2)−N(4)	126.15(12)	Ta(1)−N(1)−C(19)	115.6(3)
Ta(2)−N(4)	2.235(3)	N(3)−Ta(2)−P(2)	79.58(9)	Ta(1)−N(1)−Si(1)	129.12(19)
Ta(2)−P(2)	2.5796(9)	N(4)−Ta(2)−P(2)	82.00(8)	C(19)−N(1)−Si(1)	115.1(3)
Ta(2)−P(3)	2.5919(9)	N(3)−Ta(2)−P(3)	93.67(9)	Ta(1)−N(2)−C(13)	126.0(3)
Ta(2)−Ta(1)	2.6778(3)	N(4)−Ta(2)−P(3)	139.79(9)	Ta(1)−N(2)−Si(2)	122.18(19)
Ta(1)−N(2)	2.070(3)	P(2)−Ta(2)−P(3)	102.49(4)	C(13)−N(2)−Si(2)	111.6(3)
Ta(1)−N(1)	2.169(3)	N(2)−Ta(1)−N(1)	102.07(13)	Ta(2)−N(3)−C(31)	123.7(3)
Ta(1)−C(48)	2.199(4)	N(2)−Ta(1)−N(4)	163.43(12)	Ta(2)−N(3)−Si(3)	127.19(18)
Ta(1)−N(4)	2.410(3)	N(1)−Ta(1)−N(4)	93.77(12)	C(31)−N(3)−Si(3)	109.1(3)
Ta(1)−P(1)	2.6318(9)	N(2)−Ta(1)−P(1)	85.35(10)	Ta(2)−N(4)−C(43)	89.2(2)
		N(1)−Ta(1)−P(1)	78.30(10)	Ta(2)−N(4)−Si(4)	115.10(16)
		N(4)−Ta(1)−P(1)	93.22(8)	C(43)−N(4)−Si(4)	122.0(3)

Table 2. Crystallographic Data and Details of Refinement

	4a	4b
empirical formula	$C_{60}H_{92}N_4Si_4P_3Ta_2$	$C_{54}H_{72}N_4P_3Si_4Ta_2$
fw	1436.55	1345.43
cryst syst	triclinic	monoclinic
space group	$P\bar{1}$	$P2_1/n$
$a-c$ (Å)	11.2799(2), 13.4464(4), 22.9421(7)	11.1558(8), 23.4870(16), 22.5891(17)
α, β, γ (deg)	81.286(4), 77.613(4), 73.064(4)	90.0, 84.011(4), 90.0
V, Å^3	3236.53(48)	5886.4(7)
Z	2	4
D_{calc}, g cm^{-3}	1.37	1.517
μ(Mo Kα), cm^{-1}	3.559	3.915
T, K	173 ± 1	173 ± 1
2θ range (deg)	55.76	60.04
total reflns	25 544	19 536
unique reflns	18 249	11 663
parameters	673	615
R_1[a]	0.0330	0.0554
R_w[a]	0.0705	0.0963
goodness-of-fit	1.134	1.038

[a] $R_1 = \Sigma||F_o| - |F_c||/\Sigma|F_o|$; $R_w = \Sigma w(|F_o^2| - |F_c^2|)^2/\Sigma w|F_o^2|^2)^{1/2}$.

The structure shows two ^{CyPh}[NPN] ligands and a single PMe_3 group consistent with the $^{31}P\{^1H\}$ NMR data. However, the lack of symmetry arises from an N−Ph ring that has undergone C−H activation to generate a Ta[μ-N(C_6H_4)]Ta moiety. Relevant bond lengths and angles are listed in Table 1, and crystallographic data are located in Table 2. The Ta1−C48 distance of 2.199(4) Å is within standard Ta−C bond lengths. The amido donor attached to this ring appears to be bridging the two tantalum centers. Amido donors N1, N2, and N3 are planar; the sum of angles around each are 359.82°, 359.78°, and 359.99°, respectively. The unique amido nitrogen, N4, is pyramidal, with the sum of angles Ta2−N4−Si4, C43−N4−Si4, and C43−N4−Ta2 being 326.3°. Therefore, the amido lone pair on N4 is not π-donating to Ta2, but rather is directed at Ta1. The Ta1−N4 distance of 2.410(3) Å is quite long, much longer than the Ta2−N4 bond length of 2.235(3) Å; nevertheless, the orientation and distance still support a bridging amide.

The terminal hydride was located in the diffraction pattern and refined isotropically. H101 is located on the same Ta center as the PMe_3 group, between N4, P3, and P2 donors. Unfortunately, no evidence for the bridging hydrides could be found in the diffraction pattern, although calculated positions were suggested with the use of X-HYDEX.[17] On the basis of the observed diamagnetism and using oxidation state formalisms, complex **4a** is a Ta(IV)−Ta(IV) dimer with a Ta−Ta single bond. The Ta1−Ta2 interatomic distance of 2.6778(3) Å is in the range reported for single Ta−Ta bonds.[6,13,18−21]

The formation of this cyclometalated product likely results from dissociation of one PMe_3 from the intermediate dinuclear dihydride **3a**, which opens up a site for the ortho-hydrogen of an N−Ph to undergo C−H activation across the Ta=Ta double bond (Scheme 1). Attempts to determine the origin of the terminal hydride with isotopic labeling studies were inconclusive. Employing (^{CyPh}[NPN]Ta)$_2$(μ-D)$_4$ in an analogous experiment showed isotopic mixing across all three hydridic resonances; integration of $^1H\{^{31}P\}$ NMR peaks for H_A, H_B, and H_C summed to ∼1H, supporting orthometalation followed by isotopic mixing to form three isotopomers. We have not seen any evidence of dissociation into mononuclear fragments for any of this chemistry; for example, mixing **1a** and **1b** did not produce any cross products indicative of fragmentation.

While the formation of **4a** needed to be encouraged by the removal of H_2 in vacuo, the same transformation of the phenylphosphine-substituted tetrahydride (^{PhPh}[NPN]Ta)$_2$(μ-H)$_4$, **1b**, with PMe_3 proved more facile. Addition of just 1 equiv of PMe_3 to an ethereal solution of **1b** promoted an instantaneous color change from purple to red. Analysis of the product showed it was similar to the orthometalated complex **4a**. $^{31}P\{^1H\}$ NMR spectra showed three resonances at −18.25 (d), 6.18 (s), and 10.87 (d) ppm, respectively. As in **4a**, three hydride resonances were observed (11.46, 8.41, and 5.29 ppm). Integration of the peaks between −0.5 and 0.8 ppm indicated eight silylmethyl resonances and one coordinated PMe_3. 2D NMR experiments clearly indicated orthometalation of a ligand phenyl ring, analogous to that observed in **4a**; however, it was uncertain whether the N−Ph or P−Ph ring had undergone C−H activation.

X-ray quality crystals containing 0.5 equiv of cocrystallized solvent were grown from the slow evaporation of a benzene solution of the crude product. Analysis of these crystals by X-ray crystallography confirmed the formation of the analogous C−H activated product to **4a**, namely, ^{PhPh}[NPN]Ta(μ-H)$_2$[μ-N(C_6H_4)]Ta[PN](H)(PMe_3), **4b**. An ORTEP[16] depiction of the solid-state molecular structure of **4b** is shown in Figure 2 (see also eq 3).

(16) Farrugia, L. J. *J. Appl. Crystallogr.* **1997**, *30*, 565.

(17) Orpen, A. G. *J. Chem. Soc., Dalton Trans.* **1980**, 2509.

Scheme 1

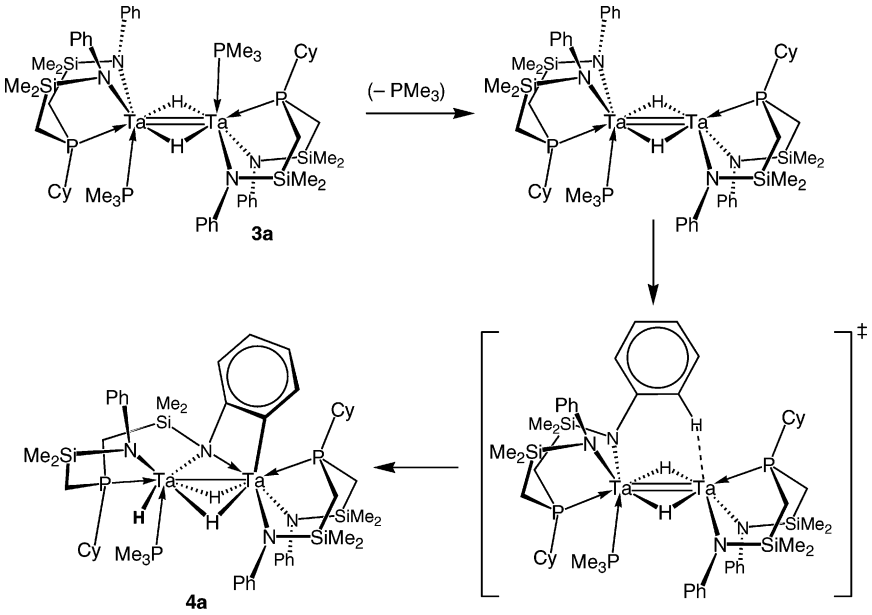

Table 3. Selected Bond Distances (Å) and Angles (deg) for 4b

lengths		angles		angles	
Ta(2)–N(3)	2.140(8)	N(3)–Ta(2)–N(4)	126.4(3)	Ta(1)–N(1)–C(22)	117.9(6)
Ta(2)–N(4)	2.223(7)	N(3)–Ta(2)–P(2)	80.1(2)	Ta(1)–N(1)–Si(1)	128.3(4)
Ta(2)–P(2)	2.570(3)	N(4)–Ta(2)–P(2)	81.8(2)	C(22)–N(1)–Si(1)	113.6(7)
Ta(2)–P(3)	2.593(2)	N(3)–Ta(2)–P(3)	92.0(2)	Ta(1)–N(2)–C(16)	123.0(5)
Ta(2)–Ta(1)	2.6689(5)	N(4)–Ta(2)–P(3)	140.8(2)	Ta(1)–N(2)–Si(2)	124.8(4)
Ta(1)–N(2)	2.079(8)	P(2)–Ta(2)–P(3)	99.94(8)	C(16)–N(2)–Si(2)	112.1(6)
Ta(1)–N(1)	2.145(8)	N(2)–Ta(1)–N(1)	103.7(3)	Ta(2)–N(3)–C(34)	122.6(9)
Ta(1)–C(45)	2.167(11)	N(2)–Ta(1)–N(1)	103.7(3)	Ta(2)–N(3)–Si(3)	127.5(5)
Ta(1)–N(4)	2.353(8)	N(2)–Ta(1)–N(4)	156.2(3)	C(34)–N(3)–Si(3)	109.9(6)
Ta(1)–P(1)	2.618(2)	N(1)–Ta(1)–N(4)	97.3(3)	Ta(2)–N(4)–C(40)	88.4(5)
		N(2)–Ta(1)–P(1)	84.0(2)	Ta(2)–N(4)–Si(4)	117.1(4)
		N(1)–Ta(1)–P(1)	79.5(2)	C(40)–N(4)–Si(4)	120.0(7)
		N(4)–Ta(1)–P(1)	88.98(17)	Ta(2)–N(4)–Ta(1)	71.3(2)

Relevant bond lengths and angles are listed in Table 3, and crystallographic data are located in Table 2. The structures of **4a** and **4b** are quite similar. The Ta(1)–C(45) distance in **4b** is 2.167(11) Å and the Ta(1)–Ta(2) distance is 2.6689(5) Å, both differing only slightly from previously observed bond lengths. The Ta(1)–N(3) and Ta(2)–N(3) distances of 2.353(8) and 2.223(7) Å, respectively, indicate a more symmetrical bridging by the amido ligand. This is again supported by the planarity of N(1), N(2), and N(3) in comparison to N(4); the sum of angles around N(4) is 326.2°. Unfortunately, none of the hydrides were located within the diffraction pattern due to the low quality of the crystal. Three hydrides were located in the diffraction pattern by X-HYDEX:[17] one terminally bound to Ta(2) and two located bridging the tantalum centers.

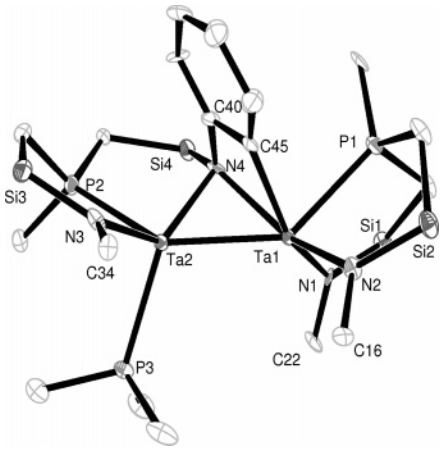

Figure 2. ORTEP drawing (spheroids at 50% probability) of **4b**. Silylmethyl and N- and P-phenyl ring carbons other than ipso carbons have been omitted for clarity.

Changing the phosphine donor from cyclohexyl to the inferior σ-donor phenyl drastically increases the proclivity for the orthometalation reaction to occur. Presumably, the cyclohexyl phosphine donor better stabilizes the reactive intermediates, and ligand decomposition is less favorable.

Attempts to characterize decomposition products in the absence of phosphine traps have been unsuccessful. Exposing **1a** and **1b** to vacuum at low concentrations did result in a purple to brown color change, but analysis of this crude material indicated a myriad of products due to decomposition. This observation, however, helps to explain previous observations[2] in the synthesis of the side-on end-on dinitrogen complex $({}^{PhPh}[NPN]Ta)_2(\mu\text{-}\eta^1{:}\eta^2\text{-}N_2)(\mu\text{-}H)_2$. It was noted that the yields and purity of this complex dramatically improved when reaction with dinitrogen is conducted under a 90/10 N_2/H_2 mixture instead of a pure N_2 atmosphere. The activation of N_2 by **1b** is a slow reaction and

is hindered further by the low solubility of molecular nitrogen in diethyl ether or toluene. The presence of H_2 in the system kinetically stabilizes the dihydride species **2b**, swinging the equilibrium toward the relatively stable tetrahydride complex **1b** (eq 1). With the concentration of reactive Ta=Ta bonds low, the poor solubility of N_2 in the reaction solvent is marginalized, and the decomposition reaction is minimized.

Concluding Remarks

The results of this study provide further experimental evidence for the intermediacy of the reactive dinuclear dihydride species $(^{RPh}[NPN]Ta)_2(\mu\text{-}H)_2$ in the activation of small molecules by the highly reducing tetrahydride $(^{RPh}[NPN]Ta)_2(\mu\text{-}H)_4$ (R = Cy, **1a**; R = Ph, **1b**). The addition of PMe_3 to **1a** at low temperatures results in a color change from deep purple to green, and spectroscopic evidence is consistent with the formation of $(^{CyPh}[NPN]Ta(PMe_3))_2(\mu\text{-}H)_2$ (**3a**). However, **3a** is unstable except at low temperatures, and upon warming under vacuum, one of the N−Ph substituents is orthometalated to generate $^{CyPh}[NPN]Ta(\mu\text{-}H)_2[\mu\text{-}N(C_6H_4)]Ta[PN](H)(PMe_3)$, **4a**. This same transformation is obtained upon addition of PMe_3 to $(^{PhPh}[NPN]Ta)_2(\mu\text{-}H)_4$, **1a**; however, in this case the formation of $^{PhPh}[NPN]Ta(\mu\text{-}H)_2[\mu\text{-}N(C_6H_4)]Ta[PN](H)(PMe_3)$, **4b**, occurs rapidly and with no detectable PMe_3 intermediates. Such an effect of the substituent at phosphorus in the NPN ancillary ligand backbone is likely due to the ability of the more electron rich $^{CyPh}[NPN]$ system to stabilize the dinuclear dihydride **2a**. Orthometalation of ancillary N−Ph amide ligands is rare to our knowledge; typically, cyclometalation of ortho-substituted ligands is more common.[22−24]

Experimental Section

General Considerations. Unless otherwise stated, all manipulations were performed under an inert atmosphere of dry, oxygen-free dinitrogen or argon by means of standard Schlenk or glovebox techniques. Where choice of atmosphere affects reaction outcomes, the distinction between dinitrogen and argon will be made. Anhydrous hexanes and toluene were purchased from Aldrich, sparged with dinitrogen, and passed through activated alumina and Ridox catalyst columns under a positive pressure of nitrogen prior to use.[25] Anhydrous pentane, benzene, tetrahydrofuran, and diethyl ether were purchased from Aldrich, sparged with dinitrogen, and passed through an Innovative Technologies Pure-Solv 400 solvent purification system. All organic solvents were tested with addition of a toluene solution of sodium benzophenone ketyl prior to use to ensure absence of oxygen and water. Alternatively, anhydrous diethyl ether was stored over sieves and distilled from sodium benzophenone ketyl under argon. Tetrahydrofuran was refluxed over CaH_2 prior to distillation from sodium benzophenone ketyl under argon, and pentane was stored over sieves and distilled from sodium benzophenone ketyl solubilized by tetraglyme under argon prior to storage over a potassium mirror. Nitrogen gas was dried and deoxygenated by passage through a column containing activated molecular sieves and MnO. Deuterated benzene was dried by heating at reflux with sodium/potassium alloy in a sealed vessel under partial pressure, then trap-to-trap distilled, and freeze−pump−thaw degassed three times. Unless otherwise stated, ^1H, ^{31}P, $^1H\{^{31}P\}$, and $^{31}P\{^1H\}$ NMR spectra were recorded on a Bruker AMX-500 instrument with a 5 mm BBI probe operating at 500.1 MHz for ^1H. ^1H NMR spectra were referenced to residual protons in C_6D_5H (δ 7.15 ppm) with respect to tetramethylsilane at δ 0.0 ppm. ^{31}P NMR spectra were referenced to either external or internal $P(OMe)_3$ (δ 141.0 ppm with respect to 85% H_3PO_4 at δ 0.0 ppm). Elemental analyses were performed by Mr. M. Lakha of the University of British Columbia, Department of Chemistry. Complexes $(^{PhPh}[NPN]Ta)_2(\mu\text{-}H)_4$[2] and $(^{CyPh}[NPN]Ta)_2(\mu\text{-}H)_4$[5] were prepared by literature procedures. PMe_3 was purchased from Aldrich and distilled under N_2 prior to use.

Reaction of $(^{CyPh}[NPN]Ta)_2(\mu\text{-}H)_4$ with Excess PMe_3. A solution of PMe_3 (29.0 mg, 0.381 mmol) in d_8-toluene (1.5 mL) was vacuum transferred into a sealable NMR tube containing $(^{CyPh}[NPN]Ta)_2(\mu\text{-}H)_4$ (50.0 mg, 0.0381 mmol). The NMR tube was sealed under vacuum and allowed to warm to room temperature briefly, and then cooled back to −78 °C, promoting a color change from deep purple to dark green. The crude mixture was analyzed by low-temperature $^{31}P\{^1H\}$ and $^1H\{^{31}P\}$ NMR spectroscopy. ^1H NMR (C_7D_8, −80 °C, 500 MHz, selected resonance): 8.5 (br, 2H, Ta*H*Ta). $^{31}P\{^1H\}$ NMR (C_7D_8, −80 °C, 202.5 MHz): δ −62 (s, in excess), −30 (br, 2P), 18 (br, 2P), 29 (br, in excess).

Synthesis of $^{CyPh}[NPN]Ta(\mu\text{-}H)_2[\mu\text{-}N(C_6H_4)]Ta[PN](H)(PMe_3)$, 4a. A solution of PMe_3 (290.0 mg, 3.81 mmol) in Et_2O (50 mL) was vacuum transferred into a vessel containing $(^{CyPh}[NPN]Ta)_2(\mu\text{-}H)_4$ (500.0 mg, 0.381 mmol). The contents of the flask were frozen, and the vessel was evacuated and sealed. Allowing the contents to warm to room temperature, followed by stirring for 1 h, promoted a color change from deep purple to red. Removal of volatiles after 2 h gave a dark red powder, which was dissolved in benzene. Slow evaporation of the benzene solution gave crystals (85%) of **4a** suitable for X-ray diffraction. $^1H\{^{31}P\}$ NMR (C_6D_6, 25 °C, 500 MHz): δ −0.34, 0.17, 0.16, 0.03, 0.18, 0.27, 0.53, 0.72 (s, 24H total, SiCH_3), 0.36 (s, 9H, P(CH_3)$_3$), 0.08−1.75 (m, 30H, PCH_2, PC$_6H_{11}$), 5.06 (d, 1H, Ta*H*), 6.55−7.63 (m, 19H, NPh-*H*), 8.15 (s, 1H, Ta*H*), 11.24 (d, 1H, Ta*H*). $^{31}P\{^1H\}$ NMR (C_6D_6, 25 °C, 202.5 MHz): δ −20.2 (d, $^2J_{PP}$ = 188 Hz, *P*Me$_3$), 10.5 (s, N*P*N), 13.8 (d, $^2J_{PP}$ = 18.8 Hz, N*P*N). ^1H,^{31}P HSQC: $^{31}P\{^1H\}$ δ −20.2 (0.36, 5.06), 10.5 (0.18, 0.27, 1.09−1.75, 8.15), 13.8 (−0.17, 0.03, 1.09−1.75, 11.24). ^1H,^1H COSY (selected correlations): δ 7.63 (β, 7.48), 7.48 (α, 7.63; δ, 6.76), 6.76 (β, 7.48; γ, 6.55), 6.55 (δ, 6.76). Anal. Calcd for $C_{51}H_{85}N_4P_3Si_4Ta_2$: C, 46.36; H, 6.48; N, 4.24. Found: C, 46.80; H, 6.81; N, 4.02.

Synthesis of $^{PhPh}[NPN]Ta(\mu\text{-}H)_2[\mu\text{-}N(C_6H_4)]Ta[PN](H)(PMe_3)$, 4b. A solution of PMe_3 (29.3 mg, 0.385 mmol) in Et_2O (50 mL) was vacuum transferred into a vessel containing $(^{PhPh}[NPN]Ta)_2(\mu\text{-}H)_4$ (500.0 mg, 0.385 mmol). Allowing the contents to warm to room temperature promoted an immediate color change from deep purple to red. Removal of volatiles after 30 min gave a dark red powder, which was dissolved in toluene. Removal of solvent gave **4b** in >85% yield. Slow evaporation of a benzene solution of **4b** gave crystals suitable

(18) Profilet, R. D.; Fanwick, P. E.; Rothwell, I. P. *Polyhedron* **1992**, *11*, 1559.
(19) Fryzuk, M. D.; Johnson, S. A.; Rettig, S. J. *Organometallics* **2000**, *19*, 3931.
(20) Chadeayne, A. R.; Wolczanski, P. T.; Lobkovsky, E. B. *Inorg. Chem.* **2004**, *43*, 3421−3431.
(21) Miller, R. L.; Toreki, R.; LaPointe, R. E.; Wolczanski, P. T.; van Duyne, G. D.; Roe, D. C. *J. Am. Chem. Soc.* **1993**, *115*, 5.
(22) Chesnut, R. W.; Jacob, G. G.; Yu, J. S.; Fanwick, P. E.; Rothwell, I. P. *Organometallics* **1991**, *10*, 321−8.
(23) Abbenhuis, H. C. L.; Van Belzen, R.; Grove, D. M.; Klomp, A. J. A.; Van Mier, G. P. M.; Spek, A. L.; Van Koten, G. *Organometallics* **1993**, *12*, 210−19.
(24) Kawaguchi, H.; Matsuo, T. *J. Am. Chem. Soc.* **2003**, *125*, 14254−14255.
(25) Pangborn, A. B.; Giardello, M. A.; Grubbs, R. H.; Rosen, R. K.; Timmers, F. J. *Organometallics* **1996**, *15*, 1518.

for X-ray diffraction. $^1H\{^{31}P\}$ NMR (C_6D_6, 25 °C, 500 MHz): δ −0.30, −0.12, −0.10, 0.09, 0.23, 0.33, 0.42, 0.58 (s, 24H total, $SiCH_3$), 0.40 (s, 9H, $P(CH_3)_3$), 1.11−2.26 (m, 8H, PCH_2), 5.29 (d, 1H, Ta*H*), 6.51−7.67 (m, 19H, NPh-*H*, PPh-*H*), 8.41 (s, 1H, Ta*H*), 11.46 (d, 1H, Ta*H*). $^{31}P\{^1H\}$ NMR (C_6D_6, 25 °C, 202.5 MHz): δ −18.25 (d, $^2J_{PP}$ = 19.1 Hz, PMe_3), 6.18 (s, N*P*N), 10.87 (d, $^2J_{PP}$ = 19.1 Hz, N*P*N). $^1H,^{31}P$ HSQC: $^{31}P\{^1H\}$ δ −18.25 (0.40, 5.29), 6.18 (0.23, 0.33, 1.11−1.58, 8.41), 10.87 (−0.12, 0.09, 1.11−1.58, 11.46). $^1H,^1H$ COSY (selected correlations): δ 7.67 (β, 7.35), 7.35 (α, 7.67; δ, 6.88), 6.88 (β, 7.35; γ, 6.51), 6.51 (δ, 6.88). Anal. Calcd for $C_{51}H_{73}N_4P_3Si_4Ta_2$: C, 46.78; H, 5.62; N, 4.28. Found: C, 47.05; H, 5.99; N, 4.14.

X-ray Crystal Structure Experimental Information. Suitable crystals were selected and coated in Paratone-N oil or an acceptable substitute under an inert atmosphere. Crystals were then mounted on a glass fiber external to the glovebox environment. All measurements were made on a Rigaku/ADSC CCD area detector with graphite-monochromated Mo Kα radiation. Diffraction data for compounds **4a** and **4b** were collected at a temperature of −100 ± 1 °C. The data were processed using the d*TREK program[26] in the CrystalClear software package (v. 1.3.5) and corrected for Lorentz and polarization effects and absorption. Neutral atom scattering factors for all non-hydrogen atoms were taken from Cromer and Waber.[27] Anomalous dispersion effects were included in F_{calc}.[28] The structures were solved by direct methods using SIR92[29] or SIR2002[30] and expanded using Fourier techniques. All non-hydrogen atoms were refined anisotropically using SHELXL-97.[31] When hydrogen atom locations were important to determine compound composition or connectivity, hydrogen atoms were located and refined isotropically. Otherwise, hydrogen atoms were included in fixed positions. Their positional parameters were calculated with fixed C−H bond distances of 0.99 Å for sp^2 C, 0.98 Å for sp^3 C, and 0.95 Å for aromatic sp C, with U_{iso} set to 1.2 times U_{eq} of the attached sp or sp^2 C and 1.5 times the U_{eq} values of the attached sp^3 C atoms. Methyl hydrogen torsion angles were determined from electron density. Structure solution and refinements were conducted using the WinGX software package, version 1.64.05.[32]

Acknowledgment. We thank NSERC of Canada for funding (Discovery Grant to M.D.F., PGS B Scholarship to M.P.S.). M.P.S. was also supported by a Killam Predoctoral Fellowship and a Li Tse Fong Fellowship. Thanks are also extended to Mr. Christopher D. Carmichael for collection of the X-ray data.

Supporting Information Available: X-ray crystallographic data for **4a** and **4b** in CIF format. This material is available free of charge via the Internet at http://pubs.acs.org.

OM050045E

(26) Pflugrath, J. W. *Acta Crystallogr.* **1999**, *D55*, 1718−1725.
(27) Cromer, D. T.; Waber, J. T. *International Tables for X-ray Crystallography*; Kynoch Press: Birmingham, 1974; Vol. IV.
(28) Ibers, J. A.; Hamilton, W. C. *Acta Crystallogr.* **1964**, *17*, 781.
(29) Altomare, A.; Burla, M. C.; Camalli, M.; Cascarano, G.; Giacovazzo, C.; Guagliardi, A.; Polidori, G. *J. Appl. Crystallogr.* **1993**, *26*, 343.
(30) Burla, M. C.; Camalli, M.; Carrozzini, G. L.; Cascarano, G. L.; Giacovazzo, C.; Polidori, G.; Spagna, R. *J. Appl. Crystallogr.* **2003**, *36*, 1103.
(31) Sheldrick, G. M. *Shelx97, Programs for Crystal Structure Analysis*; University of Gottingen: Germany, 1997.
(32) Farrugia, L. J. *J. Appl. Crystallogr.* **1999**, *32*, 837.